Novel amphibian-derived antioxidant peptide protects skin against ultraviolet irradiation damage

Chun Xie [a,1], Yan Fan [a,1], Saige Yin [a,1], Yilin Li [a], Naixin Liu [a], Yixiang Liu [b], Longjun Shu [b], Zhe Fu [a], Yinglei Wang [a], Yue Zhang [a], Xiaojie Li [c], Ying Wang [b,*], Jun Sun [a,*], Xinwang Yang [a,*]

[a] Department of Anatomy and Histology & Embryology, Faculty of Basic Medical Science, Kunming Medical University, Kunming, 650500, Yunnan, China.
[b] Key Laboratory of Chemistry in Ethnic Medicine Resource, State Ethnic Affairs Commission & Ministry of Education, School of Ethnomedicine and Ethnopharmacy, Yunnan Minzu University, Kunming, Yunnan, 650504, China.
[c] Department of Biochemistry and Molecular Biology, Faculty of Basic Medical Science, Kunming Medical University, Kunming, 650500, Yunnan, China.

ARTICLE INFO

ABSTRACT

Given the adverse impact of ultraviolet irradiation on human skin, as well as currently limited interventions, the discovery of new molecules with anti-photodamage potency remains critical. In this research, we obtained a new bioactive peptide (named OS-LL11, amino acid sequence 'LLPPWLCPRNK') from *Odorrana schmackeri*. Results showed that OS-LL11 could directly scavenge free radicals and sustain the viability of mouse keratinocytes challenged by ultraviolet B (UVB) irradiation or hydrogen peroxide (H_2O_2) by decreasing the levels of lipid peroxidation, malondialdehyde, and reactive oxygen species while increasing the level of catalase, Keap-1, HO-1, GCLM, and NQO1. Interestingly, topical application of OS-LL11 protected mouse skin against UVB irradiation damage by up-regulating the levels of superoxide dismutase, glutathione, and nitric oxide, but down-regulating the levels of H_2O_2, IL-1α, IL-1β, IL-6, TNF-α, 8-OHdG, Bcl-2, and Bax, as well as the number of apoptotic bodies. Our research demonstrated the anti-photodamage activity of a novel amphibian-derived peptide and the potential underlying mechanisms related to its free radical scavenging ability and antioxidant, anti-inflammatory, and anti-apoptotic activities. This study provides a new molecule for the development of anti-skin photodamage drugs or cosmetics and highlights the prospects of amphibian-derived peptides in photodamaged skin intervention.

1. Introduction

Exposure to sunlight can cause considerable damage to skin, including sunburn, photo-immunosuppression, photo-aging, and photo-carcinogenesis [1]. Ultraviolet (UV) radiation accounts for ~13% of sunlight, which is divided into long- (UVA: 400–315 nm), medium- (UVB: 315–280 nm), and short-wave UV light (UVC: 280–100 nm). When passing through the atmosphere, most UVC is absorbed by the ozone layer, with only UVB and UVA radiation reaching the Earth's surface [2]. UVB can penetrate the various layers of skin and cause direct

and indirect deleterious effects, such as generation of free radicals, arrest of the cell cycle, photo-aging, and photo-carcinogenesis [3]. Long-term exposure to UVB irradiation will result in the excessive accumulation of intracellular reactive oxygen species (ROS), the regulation of which is critical for maintaining normal cell homeostasis [4]. Indeed, ROS are usually maintained at a low level during normal metabolism and play an important role in many signaling processes [5,6]. Excessive ROS cannot be metabolized normally by the body due to an imbalance between oxidation and antioxidation mechanisms. Notably, excessive ROS activates various signaling pathways, including the mitogen-activated

protein kinase and nuclear factors-κB signal pathways, and attacks various biomacromolecules, such as nucleic acids, cellular proteins, and lipids, eventually leading to inflammation, apoptosis, and cytotoxicity of keratinocytes [7,8].

In recent years, the development of natural antioxidants derived from plants and animals has become an important direction in skin photodamage protection research [9]. Topical application of antioxidants is an effective way to prevent skin photo-oxidative damage. According to their molecular weight, antioxidants can be classified into two main groups, i.e., non-gene-encoded molecules with low molecular weight (e.g., vitamin C (Vc), vitamin E, and resveratrol) and gene-encoded proteins with large molecular weight (e.g., superoxide dismutase (SOD)) [10,11]. However, while antioxidants exhibit protective effects on oxidative skin damage from factors such as UV radiation, they have several disadvantages, including extended time period or large oral-administered doses, which can result in diarrhea and gastrointestinal diseases [12]. Furthermore, the application of many antioxidants is currently restricted due to their low antioxidant activity, instability, and difficulty in large-scale synthesis [13]. The use of synthetic antioxidants is also restricted because of various health risks, such as toxicity and carcinogenicity associated with overuse [14]. Therefore, the development of new antioxidants to combat oxidative damage remains an important challenge.

Amphibian skin exhibits unique characteristics that allow for exploration and survival in a wide range of habitats [15,16]. Given the vulnerability to damage from UV radiation [17], amphibian skin has evolved an excellent chemical antioxidant defense system involving the secretion of peptides with antioxidant potency [18,19]. This ability has garnered attention as these peptides can reduce oxidative damage to the skin by scavenging ROS and by stimulating the production of endogenous antioxidants [9]. Antioxidant peptides derived from amphibian skin are considered a new type of gene-encoded antioxidant, with their molecular weights falling somewhere between the non-gene-encoded low molecular weight molecules and gene-coded large molecular weight proteins [19]. Furthermore, these novel peptides provide mechanistic clues regarding how certain amphibians adapt to high-latitude surroundings with high-dose UV exposure [15]. Although many peptides have been identified from amphibians and found to exert antioxidant abilities by directly scavenging free radicals, e.g., pleurains, antioxidin-RP1 from *Rana pleuraden*, and novel antioxidant peptides (AOPs) from *Odorrana andersonii* [15,20–24], only a few show protective effects against skin photodamage, e.g., antioxidant-RL from *Odorrana livida*, AOP-P1 and OA-VI12 from *O. andersonii*, and OM-GL15 from *Odorrana margaretae* [9,25,26]. Thus, further studies are still required to explore the potential application of amphibian-derived antioxidant peptides in photodamage protection.

We previously identified many antimicrobial peptides from odorous frogs; however, given the rich diversity of peptides, we considered that they likely had other unknown structures and functions [27,28]. We recently found several odorous frog peptides that can protect the skin against UVB irradiation damage [9,29]. In the current research, a novel peptide (named OS-LL11, amino acid sequence 'LLPPWLCPRNK') was identified from *O. schmackeri* by cDNA cloning. Results showed that topical application of OS-LL11 could protect mouse skin against photodamage induced by UVB irradiation, including alleviation of erythema, desquamation, scabbing, and thickening of the epidermis and dermis. This was likely due to its direct free radical scavenging ability, antioxidant ability *in vivo* and *in vitro*, and anti-apoptotic and anti-inflammatory activities *in vivo*. Thus, our study provides a novel molecule for the development of anti-photodamage drugs or cosmetics and highlights the prospects of amphibian-derived peptides in skin photodamage interventions.

2. Material and Methods

2.1. cDNA Encoding OS-LL11

The cDNA encoding peptide OS-LL11 was obtained according to our previous report [29]. Briefly, RNA was extracted from the skin of *O. schmackeri* and the first and second strands of cDNA were synthesized using a SMART cDNA Library Construction kit (Clontech, Canada). Second strand cDNA was used as a template and two specific primers (5′-PCR primer (5′-CCAAA(G/C)ATGTTCACC(T/A)TGAAGAAA-3′) and 3′-PCR primer (5′-ATTCTAGAGGCCGAGGCGGCCGACATG-3′)) were used to screen the cDNA encoding the bioactive peptide precursor. The polymerase chain reaction (PCR) products were recovered, and sequencing was performed by Exxon Technology Co. Ltd. (Beijing, China). In brief, the PCR products (100 ng) were used for amplification with KAPA HiFi Hot Start Ready Mix (KAPA Biosystems, Beijing, China). After purification, the amplicons were quantified using a Quadit 2.0 fluorometer (Life Invitrogen, Inc., CA, USA) and sequenced on the Illumina MiSeq platform according to the standard protocols of Genetics Biotechnology (Shanghai, China). Finally, the cDNA sequence encoding OS-LL11 was obtained.

2.2. Artificial Synthesis of Peptide

The OS-LL11 peptide (LLPPWLCPRNK) was produced by Wuhan Bioyeargene Biotechnology Co., Ltd. (Wuhan, China) by solid-phase synthesis, and the purity was more than 95%. Firstly, the polypeptide was synthesized using resin, and then the Fmoc protecting group was removed with 20% piperidine/DMF solution to reveal the active NH$_2$ group. Fmoc AA was added to react with the condensing agent, and the above steps were detected and repeated until the peptide sequence was synthesized. Finally, the peptide sequence was cut from the solid phase resin and purified by high-performance liquid chromatography (HPLC).

2.3. Direct Scavenging Activities against Free Radicals

We determined the 2,2′-azino-bis (3-ethylbenzothiazoline-6-sulfonic acid) (ABTS$^+$) free radical scavenging activity of the peptide by using previously described methods [30], with minor alterations. Briefly, we incubated 7 mM ABTS (Sigma-Aldrich, USA) with 2.8 mM potassium persulfate (Sigma-Aldrich, USA) in water in the dark for 6 h to generate an ABTS$^+$ free radical stock solution. The stock solution was used immediately or stored at −20 °C for later use. We mixed 50 μL of sample and 50 μL of 125 × diluted stock solution at room temperature in the dark for 10 min, after which absorbance was measured at 415 nm by a microplate reader (Amersham Bioscience, UK). The 2,2-diphenyl-1-picrylhydrazyl (DPPH) free radical scavenging activity was determined according to prior study [31]. In brief, after mixing 190 μL of DPPH stock solution (Sigma-Aldrich, St Louis, MO, USA) with 10 μL of sample, the mixture was incubated at room temperature in the dark for 30 min. Absorbance was then measured at 517 nm using a microplate reader. In addition, ddH$_2$O was used as a negative control, and Vc was used as a positive control. The free radical scavenging rate (%) formula was: $(A_{blank} − A_{sample}) \times 100 / A_{blank}$.

2.4. Effects of OS-LL11 on Viability of Mouse Keratinocytes

The effects of OS-LL11 on the viability of mouse keratinocytes challenged with or without UVB and hydrogen peroxide (H$_2$O$_2$) were evaluated using a 3-(4,5-dimethylthiazol-2-yl)-5-4(3-carboxymethoxyphenyl)-2-(4-sulfophenyl)-2H-tetrazolium (MTS) assay kit. Briefly, mouse keratinocytes (*PAM 212* cells) were supplied by I-Cell Bioscience Inc. (Shanghai, China). Cells were cultured in Dulbecco's modified Eagle's/F12 medium (DMEM/F12, BI, Israel) with 10% fetal bovine serum (FBS, BI, Israel). The *PAM 212* cells were then seeded into 96-well plates at a density of 3.0×10^3 cells/well and cultured for 2–4 h for complete

```
ATGTTCACCTTCAAAAAATCCCTTATCATTTTCTTTTTCTTCGGTATTGTTAGTATGAGC    60

   M  F  T  L  K  K  S  L  L  L  L  F  F  F  G  I  V  S  S  S     20

GAACCTAGTTTTCGAAAACGAGATGCTGACGAAGAGGGAAATGAAGAAAATGGTGCTGAA   120

   E  P  S  F  R  K  R  D  A  D  E  E  G  N  E  E  N  G  A  E     40

GCCAAAATTGAAGAAATTATAGTGAAACGGCTTCTCCCTCCATGGCTCTGTCCACGTAAT   180

   A  K  I  E  E  I  I  V  K  R  L  L  P  P  W  L  C  P  R  N     60

AAATAATAAATTGCGATGCTGGGCCGCAGGGTATCTAAGCATGGTTCAATCTGCATGCCC   240

   K  *                                                          61

TAGAAGAGAGCGGAGAAGACGCAGGTTGCGATAGTCCTGAAATCGTAACGTCGATGCATA   300

AAAAAAAAAAAAAAAAAAA                                             318
```

Fig. 1. Sequence of cDNA encoding OS-LL11.
Precursor of OS-LL11 consisted of 61 amino acid residues and was encoded by 318-bp cDNA. Mature peptide of OS-LL11 ('LLPPWLCPRNK') is underlined and italicized.

adherence. Before irradiation with a 9 W/01/2P UVB lamp (Philips, Holland) (30 mJ/cm^2) or stimulation with 200 μM H_2O_2 (Sigma, St. Louis, Mo, USA) for 2 h, the culture medium was discarded and OS-LL11 (0.25, 0.5, and 1 μM) or 10 μM Vc (Sigma, St. Louis, MO, USA) dissolved in DMEM/F12 at a volume of 100 μL for 2 h was added to the cells, followed by 20 μL of MTS reagent (Promega, Madison, WI, USA). The cells were then cultured for 2–4 h to detect the impact of OS-LL11 and Vc on cell viability. Cell absorbance was determined with a microplate reader at 490 nm.

2.5. Effects of OS-LL11 on Lipid PerOxide (LPO), Malondialdehyde (MDA), Lactic Dehydrogenase (LDH), and Catalase (CAT) Levels in Mouse Keratinocytes

PAM 212 cells were first seeded into 6-well plates at a density of 1.2 × 10^6. Next, OS-LL11 or Vc was added to the cells for 2 h before stimulation by UVB irradiation or H_2O_2. The cells were then cultured for an additional 24 h. The culture medium was collected and centrifuged at 1000 ×*g* for 5 min at 4 °C. The resulting supernatant was used to detect the level of LDH with an LDH activity assay kit (Nanjing Jiancheng

Bioengineering Research Institute, Nanjing, China) according to the protocols provided by the manufacturer. Cell lysates were prepared using radioimmunoprecipitation assay (RIPA) lysis solution (RIPA lysate: PMSF = 100: 1, Meilun Biotechnology, Dalian, China), then centrifuged at 12000 ×*g* for 20 min at 4 °C. The resulting supernatant was used to detect LPO, MDA, and CAT levels with appropriate assay kits (Nanjing Jiancheng Bioengineering Research Institute, Nanjing) in accordance with the standard methods provided by the manufacturer. In brief, MDA in the degradation product of lipid peroxide can be condensed with thiobarbituric acid to form a red product with a maximum absorption peak at 532 nm, while one molecule of LPO can react with two molecules of chromogenic reagent at 45 °C to produce a stable chromophore with a maximum absorption peak at 586 nm. Therefore, the LPO and MDA levels were measured at 532 nm and 586 nm, respectively.

2.6. Effects of OS-LL11 on ROS Level in Mouse Keratinocytes

PAM 212 cells were seeded into 6-well plates at a density of 1.2 × 10^6, with OS-LL11 or Vc then added for 2 h, followed by UVB irradiation or H_2O_2 stimulation. The cell culture medium was refreshed and a 2′,7′-dichlorofluorescin diacetate (H$_2$DCFDA) fluorescent probe (1 mM) was added (Nanjing Jiancheng Bioengineering Research Institute, Nanjing, China), with further incubation for 45 min. The cells were digested using trypsin (BI, Israel), centrifuged at 1000 ×*g* for 5 min, and re-suspended in pre-cooled phosphate-buffered saline (PBS). The level of ROS was then detected via flow cytometry (CyFlow Space, PARTEC, Germany).

2.7. Influence of OS-LL11 on Levels of HO-1, Keap1, NQO1, and GCLM in Mouse Keratinocytes

The effects of OS-LL11 on HO-1, Keap1, NQO1, and GCLM levels in *PAM 221* cells were evaluated by western blotting. The *PAM 212* cells were seeded into 6-well plates at a density of 1.2 × 10^6, with OS-LL11 or Vc added for 2 h before UVB irradiation or H_2O_2 stimulation. The cells were then cultured for an additional 24 h. The cell lysates were prepared by the addition of RIPA lysis solution, followed by centrifugation at 12000 ×*g* for 20 min at 4 °C. The resulting supernatants were used for western blot analysis. The primary antibodies against HO-1, Keap1, NQO1, GCLM, and β-actin and secondary antibodies were commercially obtained (HO-1: cat# AF5393; Keap1: cat# AF5266; NQO1: cat# DF6437; GCLM: cat# DF7268; β-actin: cat# AF7018, Affinity Biosciences LTD. Jiangsu, China).
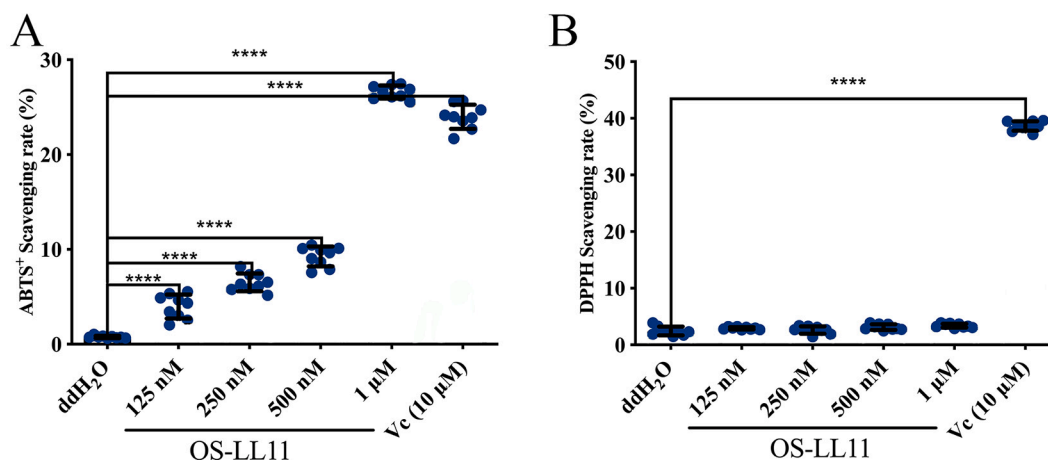
**Fig. 2.** Free radical scavenging capacity of OS-LL11.
A. OS-LL11 exerted ABTS$^+$ free radical scavenging activity.
B. OS-LL11 did not exhibit DPPH free radical scavenging activity.
ddH$_2$O was used as a negative control, Vc was used as a positive control. Data were from three independent experiments replicated three times. ****$P < 0.0001$ indicates significant difference between two groups.
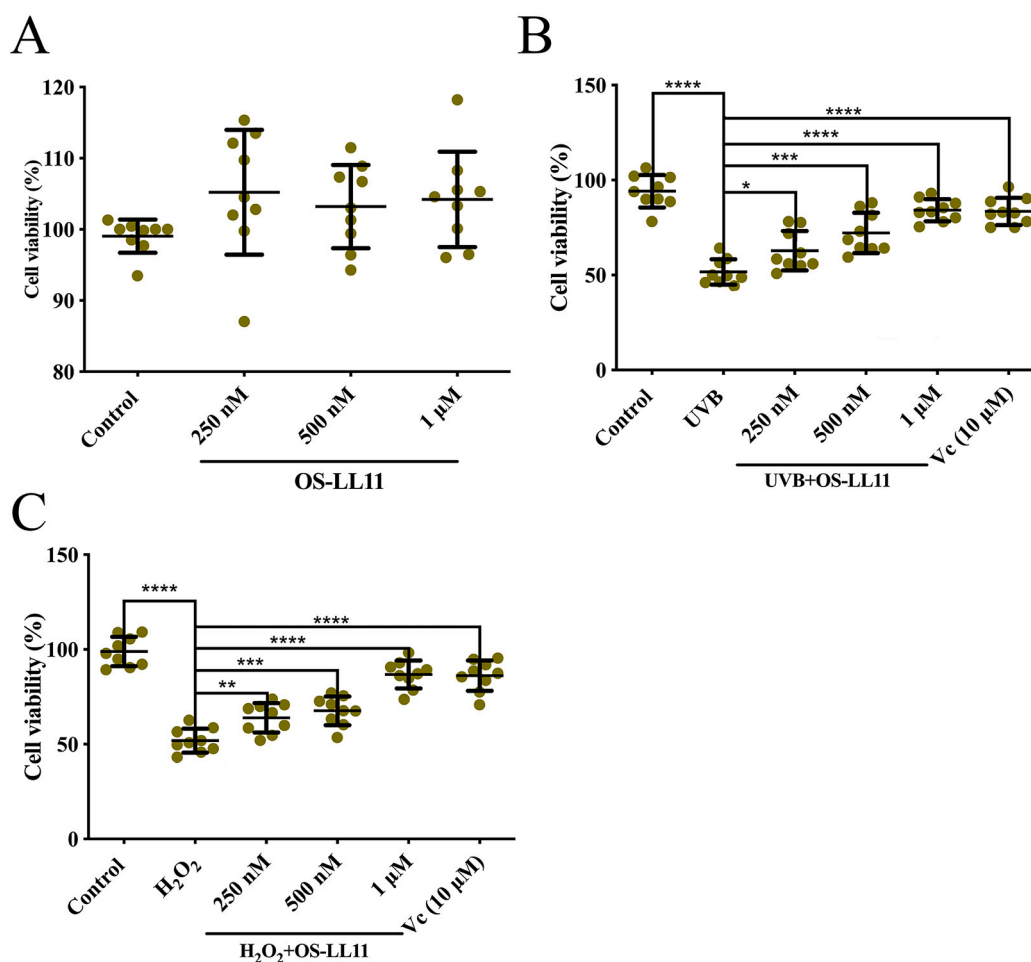
Fig. 3. Effects of OS-LL11 on *PAM 212* cell viability.

A. OS-LL11 (250 nM, 500 nM, 1 μM) showed no proliferative or toxic effects on *PAM 212* cells.

B. OS-LL11 had a protective effect against decreased viability in UVB-irradiated *PAM 212* cells.

-LL11 had a protective effect against decreased viability in H_2O_2-treated *PAM 212* cells.

Data were from three independent experiments replicated three times. *$P < 0.05$; **$P < 0.01$; ***$P < 0.001$; ****$P < 0.0001$ indicate significant differences between two groups.

2.8. Effects of OS-LL11 on UVB-Irradiated Dorsal Skin of Mice

Kunming mice (18–22 g, 3–4 weeks old, female) were purchased from Hunan Slake Jingda Experimental Co., Ltd. (Hunan, China) and acclimated to the laboratory environment for at least one week before the experiments, with free access to food and water. A mouse model of chronic skin photodamage induced by UVB irradiation was successfully constructed to evaluate the anti-photodamage potency of OS-LL11 in vivo. All procedures were approved by and operated strictly in accordance with the guidelines of the Ethics Committee of Kunming Medical University (KMMU2020074). Briefly, the dorsal skin hair was removed from mice anesthetized with chloral hydrate. The mice were then positioned 20 cm under a UVB lamp (TL20 w/12, Philips, Netherlands) and their dorsal skin was exposed to UVB irradiation at a radiant intensity of 150 mJ/cm^2 every day for one week, followed by 300 mJ/cm^2 on alternate days for two weeks [25]. UVB radiation intensity was detected by an UV radiometer (TM-213, Temars, Taiwan, China). According to the formula (P(W) = E(J) / t(s)), radiation time was ~20 min in the first week and ~ 40 min in the following two weeks. The mice were randomly divided into four groups: model group (UVB) ($n = 6$), solvent group (UVB + ddH$_2$O) ($n = 6$), sample group (UVB + 1 μM OS-LL11) ($n = 6$), and positive group (UVB + 10 μM Vc) ($n = 6$). The OS-LL11 or Vc (1 mL) solutions were topically and uniformly applied over

the irradiated skin of each mouse once per day. The dorsal skin of each mouse was photographed and recorded each day to evaluate treatment effects on the occurrence of erythema, scabbing, and scarring of the photodamaged skin. On the last day of irradiation, the mice were sacrificed by decapitation, and the middle section of the dorsal skin (2 cm^2) was collected for subsequent experiments.

2.9. Histological Analysis of UVB-Irradiated Skin in Mice

Subcutaneous tissue was removed and washed with saline, then quickly placed in an embedding box for group labeling and immersed in 4% paraformaldehyde overnight for fixation. After dehydration, transparency, wax dipping, embedding, embsectioned, and slicing, the tissues were used for hematoxylin-eosin (H&E) and Masson's trichrome staining, respectively (Solarbio, Beijing, China) according to standard protocols. Epidermal and dermal thicknesses were measured and quantified using Image J software (2.0.0-rc-69/1.52p).

2.10. Effects of OS-LL11 on SOD, Glutathione (GSH), H_2O_2, and Nitric Oxide (NO) Levels in UVB-Irradiated Skin in Mice

Mouse skin tissue was washed with pre-cooled saline, weighed, and cut using ophthalmic scissors, then ground using a glass vessel in pre-
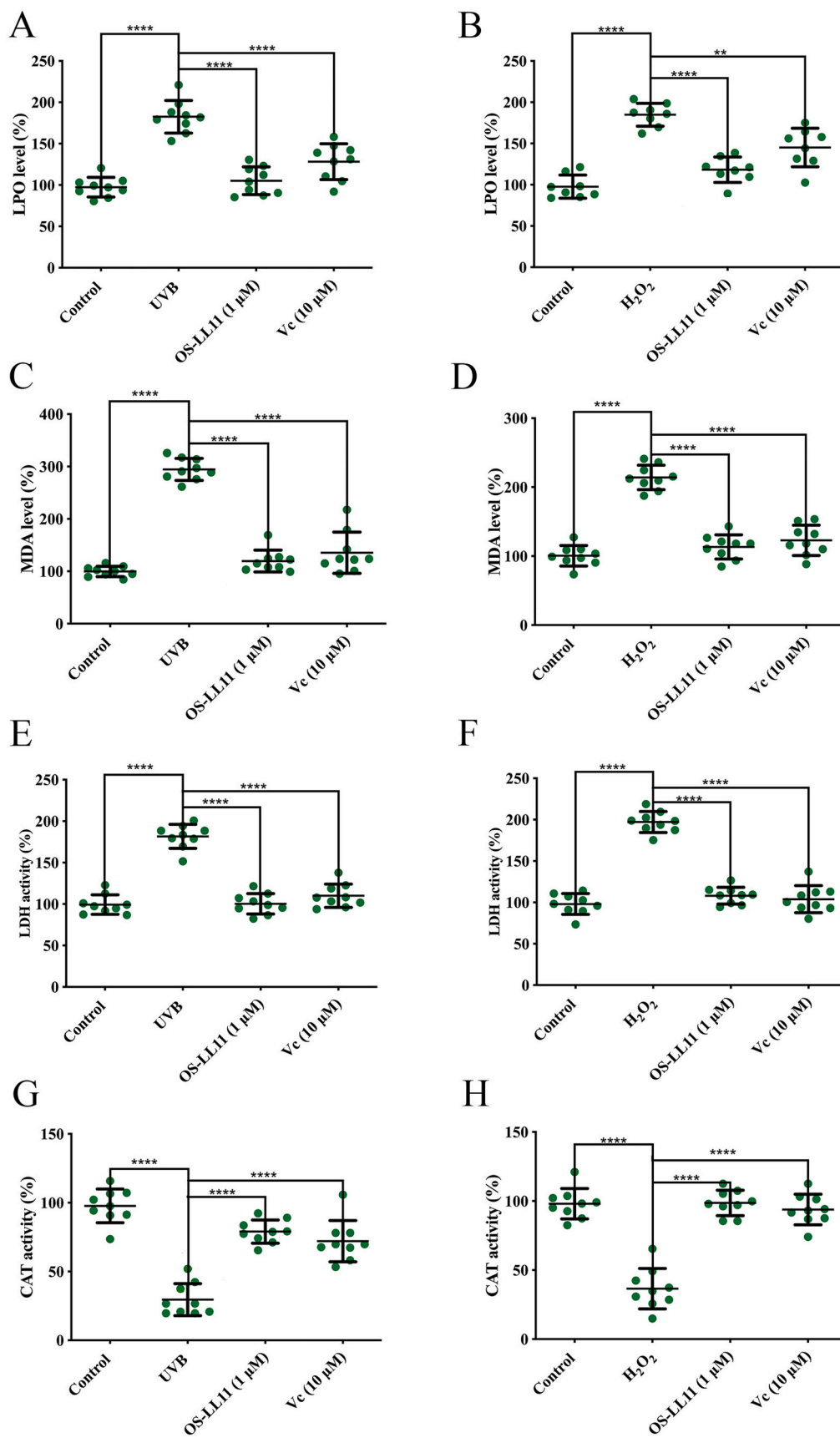
Fig. 4. Effects of OS-LL11 on LPO, MDA, LDH, and CAT levels in *PAM 212* cells stimulated by UVB or H_2O_2.

Column analysis charts of LPO levels (A, B); MDA levels (C, D); LDH levels (E, F); and CAT levels in *PAM 212* cells (G, H).

Data were from three independent experiments replicated three times. $**P < 0.01$; $****P < 0.0001$ indicate significant difference between two groups.
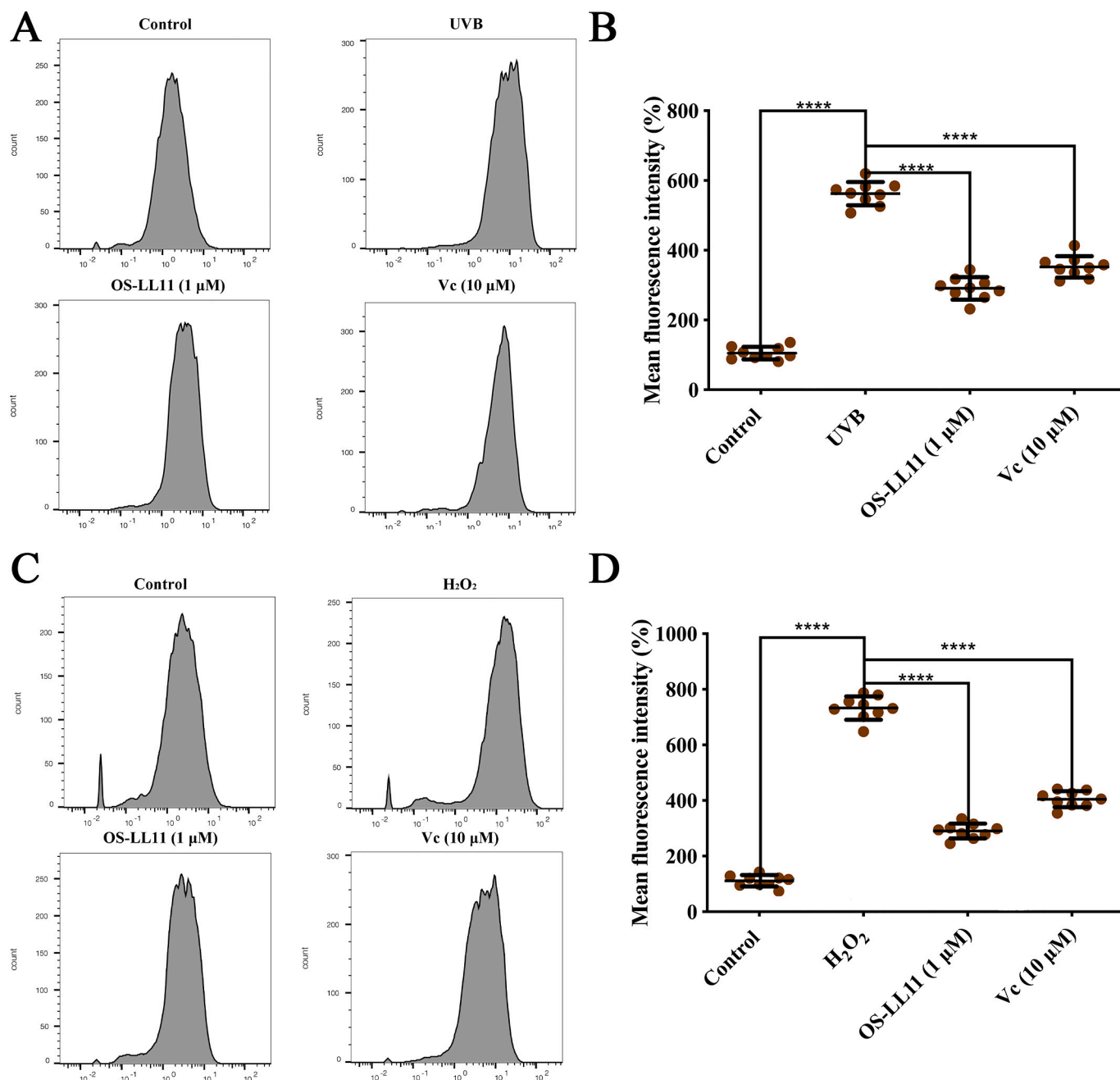
Fig. 5. Effects of OS-LL11 on levels of ROS in *PAM 212* cells stimulated with UVB or H_2O_2.

A. OS-LL11 decreased ROS levels in UVB-irradiated *PAM 212* cells.

B. Histogram of mean fluorescence intensity of ROS after UVB stimulation.

C. OS-LL11 reduced ROS levels in H_2O_2-stimulated *PAM 212* cells.

D. Histogram of mean fluorescence intensity of ROS after H_2O_2 stimulation.

Data were from three independent experiments replicated three times. ****$P < 0.0001$ indicates significant difference between two groups.

cooled saline (weight (g): volume (mL) = 1: 9). The samples were then centrifuged at 12000 ×*g* for 20 min at 4 °C and the resulting supernatants were used to detect the contents of SOD, GSH, H_2O_2, and NO. In brief, the contents of SOD, GSH, and NO were determined using appropriate kits with the WST-1, dithiol dinitrobenzoic acid, and nitrate detective methods, respectively. The three kits and protocols were provided by Nanjing Jiancheng Bioengineering Research Institute (Nanjing, China). The content of H_2O_2 was detected using the titanium peroxide complex method with a H_2O_2 assay kit (Solarbio, Beijing, China).

2.11. Effects of OS-LL11 on Inflammatory Cytokines, 8-Hydroxy-2 Deoxyguanosine (8-OHdG), BCL2-associated X (Bax), and B-Cell Lymphoma-2 (BCL-2) in UVB-Irradiated Skin in Mice

Mouse skin tissue was washed with pre-cooled saline, weighed, and cut using ophthalmic scissors, then ground using a glass vessel with pre-cooled saline (weight (g): volume (mL) = 1: 9). The samples were then centrifuged at 12000 ×*g* for 20 min at 4 °C. The resulting supernatants were used to detect the levels of IL-6, IL-1α, IL-1β, TNF-α, 8-OHdG, Bax, and Bcl-2 via enzyme-linked immunosorbent assay (ELISA) kits (Jianglai Biological Technology Co., Ltd., Shanghai, China). All procedures were
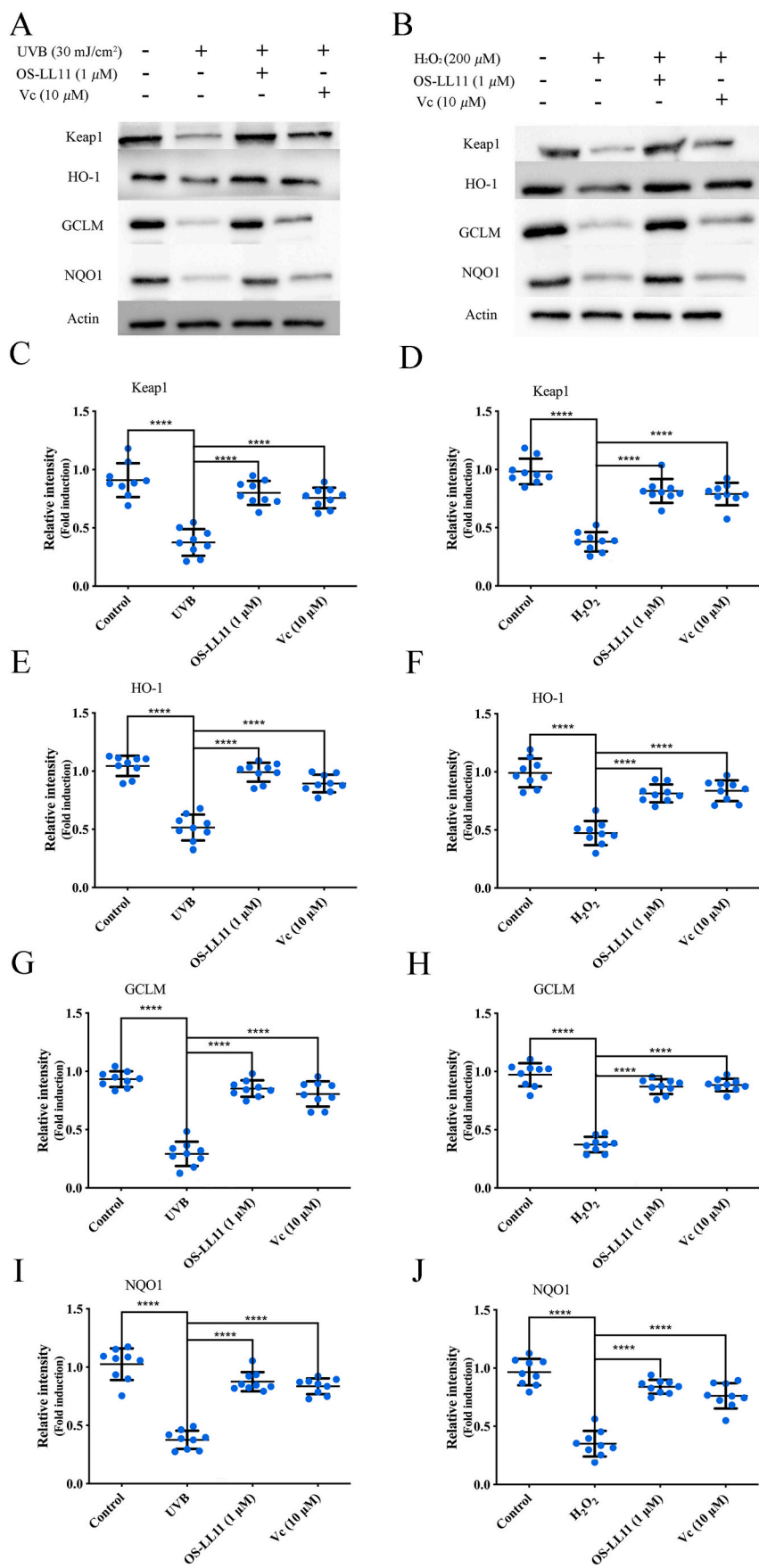
Fig. 6. Effects of OS-LL11 administration on UVB or H_2O_2-induced protein expression in *PAM 212* cells.

A, B. Cells were administered with OS-LL11 or Vc for 24 h before UVB irradiation or 200 μM H_2O_2 stimulation. Following 24 h of incubation, protein levels in cells were detected by western blot analysis. C, D, E, F, G, H, I, J. Column diagrams of protein expression levels of HO-1, Keap1, NQO1, and GCLM, respectively.

*$P < 0.05$; **$P < 0.01$; ****$P < 0.0001$ indicate significant differences.
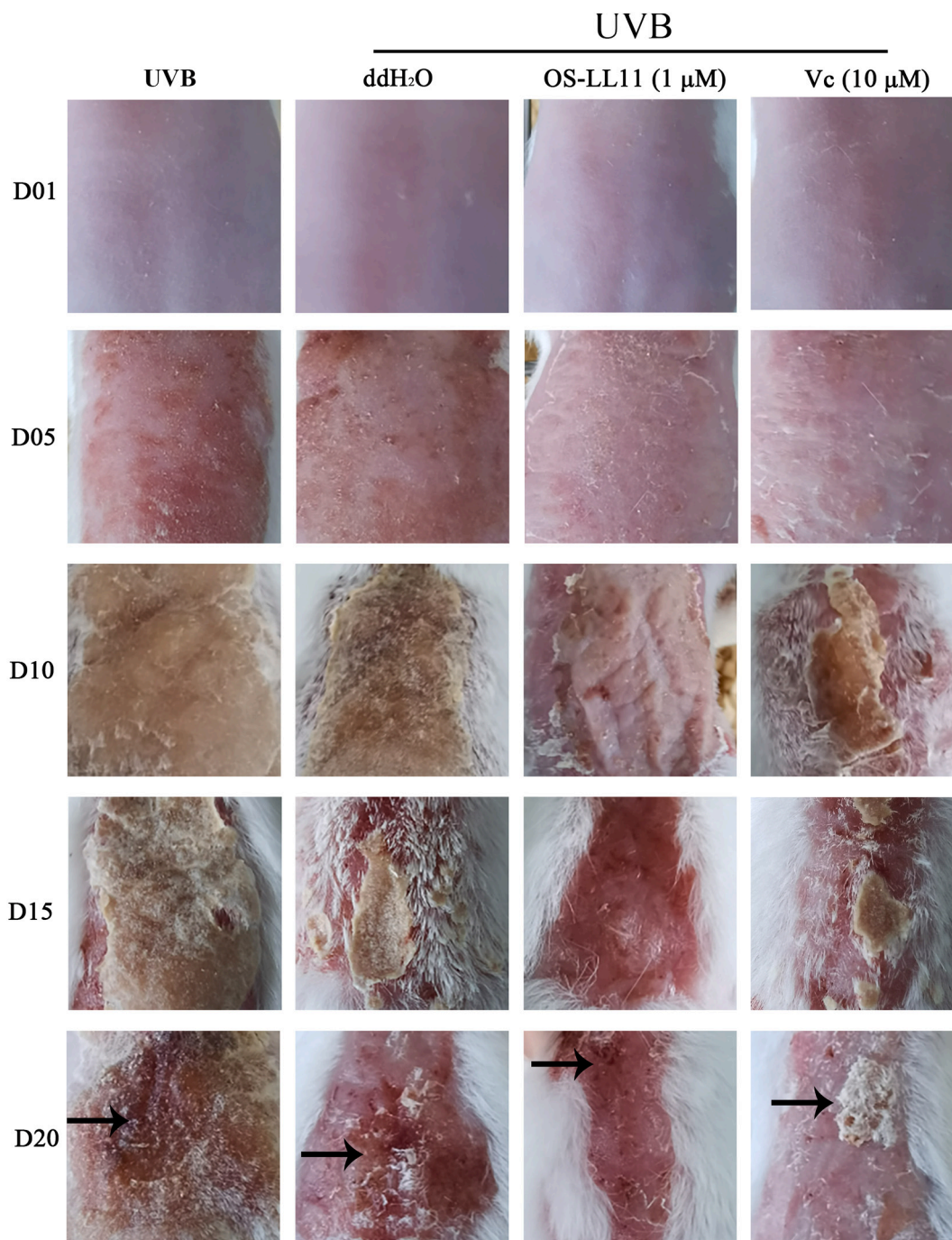
Fig. 7. Changes in dorsal skin of mice following UVB irradiation.
Surface changes in dorsal skin were recorded using photography. Arrows indicate locations of erythema, scabbing, and scarring after UVB irradiation and OS-LL11 or VC treatment.

performed in accordance with the guidelines of the manufacturer.

2.12. TUNEL Staining

After fixing in paraffin, the skin tissue samples were cut into 5–6-μm thick sections using an ultra-thin semiautomatic microtome (Leica RM2235, Wetzlar, Germany). According to standard protocols, the sections were stained using a TUNEL staining kit (Key-GEN, Jiangsu, China). Images were quantified using Image J software.

2.13. Statistical Analysis

Data are expressed as mean $\pm$ standard deviation (SD). All data are averages of at least three independent experiments. According to Duncan's test, differences between each group were measured using one-way analysis of variance (ANOVA). Values of $p < 0.05$ were considered statistically significant. All analyses were conducted using Graph-Pad Prism 9.
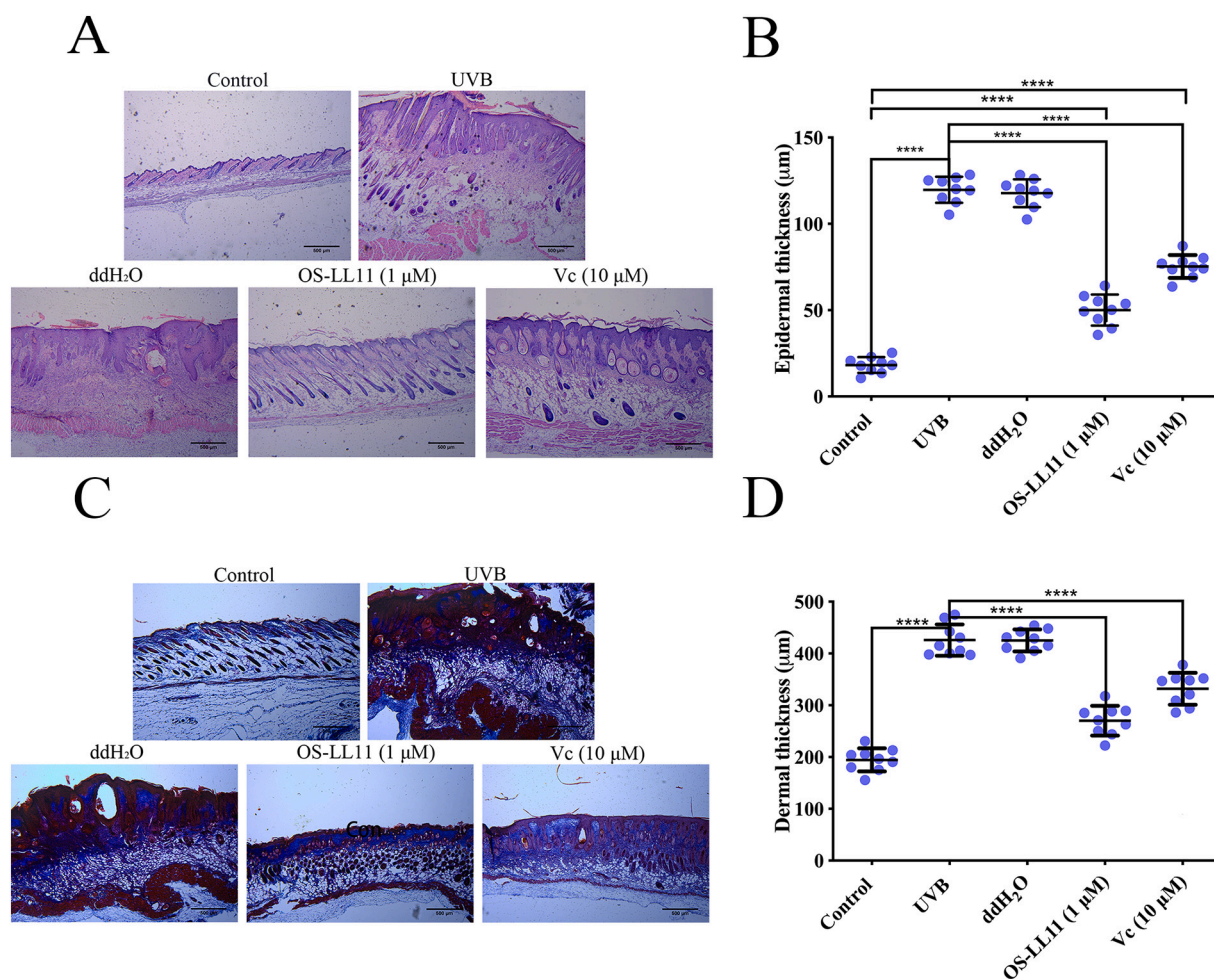
Fig. 8. Effects of OS-LL11 on epidermal and dermal thickness of dorsal skin in mice after UVB irradiation. A. Image of HE staining; B. Histogram of epidermal thickness in each group; C. Image of Masson's trichrome staining; D. Histogram of dermal thickness in each group. Scale bar: 500 μm. ****$P < 0.0001$ indicates significant differences. All data analyses were repeated three times with three replicate experiments independently.

3. Results

3.1. Identification of a Novel Peptide (OS-LL11) from Odorous Frog (O. schmackeri) Skin

As displayed in Fig. 1, a peptide precursor of 61 amino acid residues encoded by a cDNA sequence of 318 base pairs was obtained from the skin of *O. schmackeri*. The overall structure of the peptide precursor showed similarity with other known frog-derived peptides. The amino acid sequence of the mature peptide was predicted to be 'LLPPWLCPRNK' and we named the peptide OS-LL11 (OS: abbreviation of species *O. schmackeri*; LL: first and second residues; 11: number of residues). Following a BLASTp search in the NCBI database, the mature sequence was not similar to any other bioactive frog peptide, and thus was considered to represent a new peptide.

3.2. OS-LL11 Directly Scavenged Free Radicals

The cysteine, proline, and tryptophan residues indicated possible scavenging activity of OS-LL11 against free radicals. As illustrated in Fig. 2A, OS-LL11 showed direct ABTS$^+$ free radical scavenging at concentrations of 0.125, 0.25, 0.5, and 1 μM. At a concentration of 1 μM, OS-LL11 scavenged 25.82% ± 0.23% of ABTS$^+$, slightly higher than that of Vc (23.22% ± 0.43%). As shown in Fig. 2B, however, OS-LL11 showed no direct scavenging activity against DPPH.

3.3. OS-LL11 Protected against Mouse Keratinocyte Viability Decrease Induced by UVB Radiation and H$_2$O$_2$ Stimulation

OS-LL11 (0.25–1.0 μM) itself had no effect on *PAM 212* cell viability (Fig. 3A). As shown in Fig. 3B and C, both UVB irradiation and H$_2$O$_2$ treatment significantly decreased cell viability; however, OS-LL11 administration had a positive and concentration-dependent (250 nM to 1 μM) effect on keratinocyte viability. Thus, these results indicate that OS-LL11 can rescue keratinocytes from oxidative damage.

3.4. OS-LL11 Increased CAT, but Reduced LPO, MDA, LDH, and ROS Levels in Keratinocytes Stimulated by UVB and H$_2$O$_2$

As shown in Fig. 4, after UVB irradiation and H$_2$O$_2$ treatment, the levels of LPO, MDA, and LDH in *PAM 212* cells increased by 85.14% ± 7.63%, 194.90% ± 7.75%, and 82.34% ± 6.23% and by 87.12% ± 6.99%, 113.50% ± 7.71%, and 99.06% ± 5.95%, respectively. However, pretreatment with OS-LL11 decreased the levels of LPO, MDA, and LDH by 77.36% ± 8.61% (Fig. 4A), 174.90% ± 9.90% (Fig. 4C), and 81.34% ± 6.36% (Fig. 4E) and by 66.58% ± 7.34% (Fig. 4B), 100.70% ± 8.32% (Fig. 4D), and 89.03% ± 5.42% (Fig. 4F), respectively. In addition, UVB irradiation and H$_2$O$_2$ treatment decreased the level of CAT by 68.11% ± 5.63% and 61.44% ± 6.10%, respectively, while pretreatment with OS-LL11 (1 μM) increased CAT by 49.45% ± 4.80% (Fig. 4G) and 62.05% ± 5.75% (Fig. 4H), respectively.

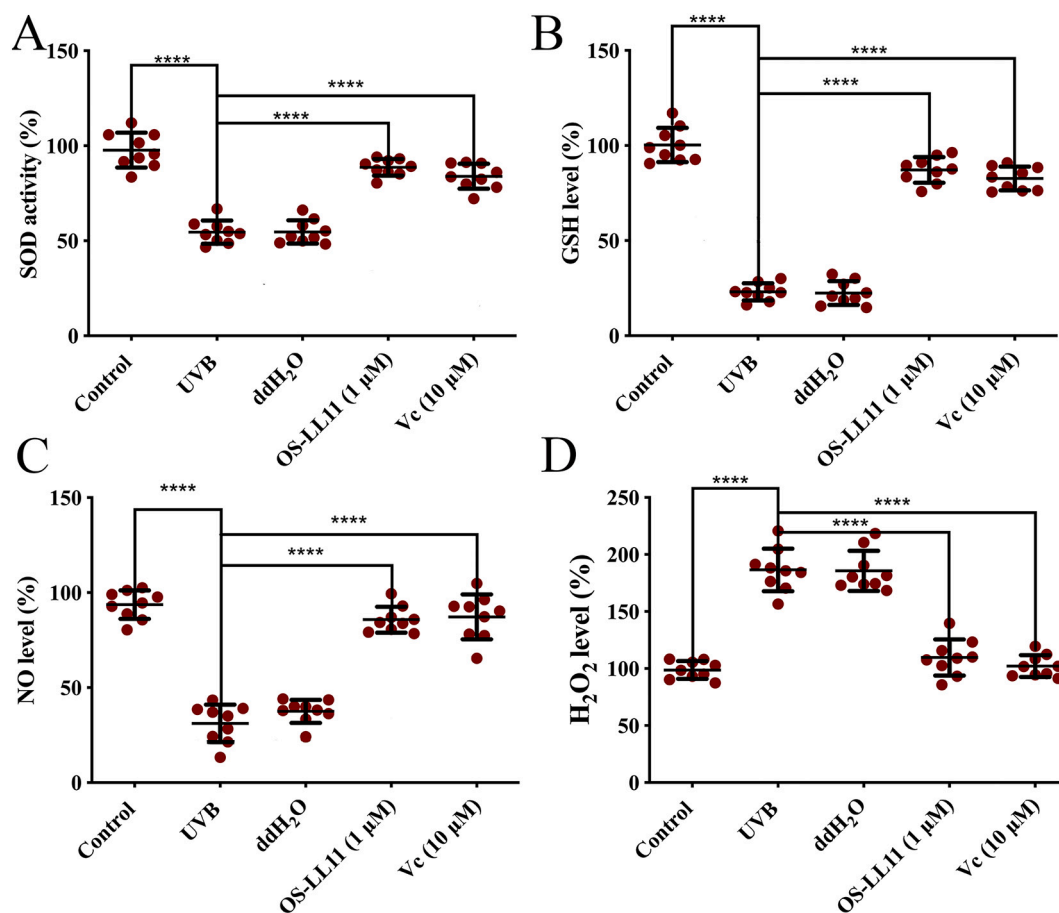After UVB irradiation/H$_2$O$_2$ treatment, the level of ROS in the *PAM*

Fig. 9. Effects of OS-LL11 on SOD, GSH, NO, and H_2O_2 levels in mouse skin following UVB irradiation.
OS-LL11 administration increased SOD levels (A); GSH levels (B); and NO levels (C) but decreased H_2O_2 levels (D). *$P < 0.05$; **$P < 0.01$; ***$P < 0.001$; ****$P < 0.0001$ indicate significant differences. All data analyses were repeated three times with three replicate experiments independently.

212 cells increased markedly compared to that in the untreated group, while application of OS-LL11 decreased the level of ROS (Fig. 5). Specifically, compared with the UVB-irradiated and H_2O_2-treated groups, OS-LL11(1 μM) reduced ROS by 271.70% ± 15.44% (Fig. 5A, B) and 442.40% ± 16.60%, respectively (Fig. 5C, D), while Vc treatment decreased ROS by 210.10% ± 15.11% and 327.80% ± 16.98%, respectively. Thus, the effect of OS-LL11 on ROS levels in *PAM 212* cells was better than that of Vc (Fig. 5C, D).

3.5. OS-LL11 Increased Expression of Oxidative Stress-Related Proteins in PAM 212 Cells

After UVB irradiation and H_2O_2 stimulation, the levels of Keap1, HO-1, GLCM, and NQO1 decreased in the *PAM 212* cells, which was reversed by OS-LL11 pretreatment (Fig. 6A, B). After UVB irradiation and H_2O_2 stimulation, the protein expression levels of Keap1, HO-1, GLCM, and NQO1 decreased by 0.42 ± 0.05 and 0.44 ± 0.04 (Fig. 6C, D), 0.48 ± 0.05 and 0.34 ± 0.04 (Fig. 6E, F), 0.56 ± 0.04 and 0.86 ± 0.03 (Fig. 6G, H), and 0.50 ± 0.04 and 0.49 ± 0.04 (Fig. 6I, J), respectively. However, the expression levels of these proteins increased by 0.57 ± 0.09 and 0.65 ± 0.11 (Keap1), 0.52 ± 0.03 and 0.33 ± 0.02 (HO-1), 0.71 ± 0.07 and 0.81 ± 0.04 (GCLM), and 0.69 ± 0.08 and 0.67 ± 0.04 (NQO1) after OS-LL11 pretreatment.
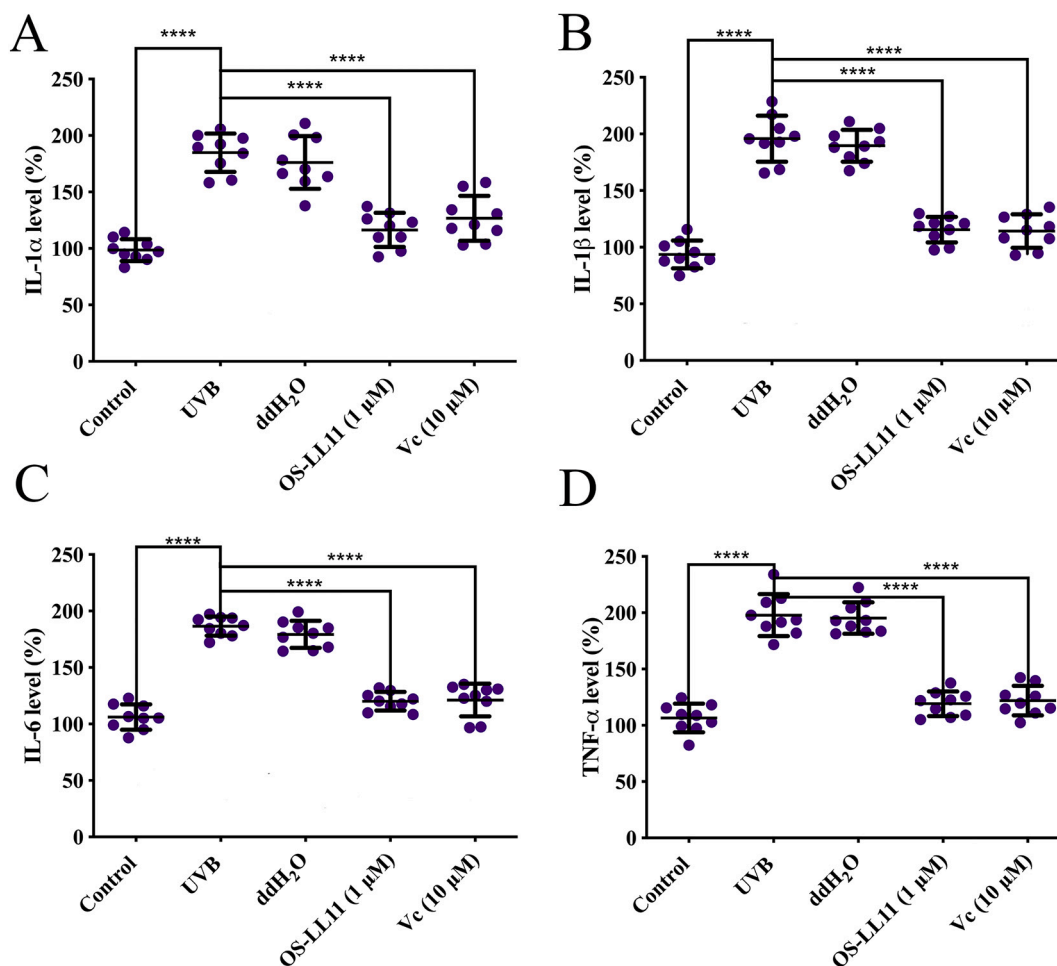
3.6. Effects of OS-LL11 on Dorsal Skin of Mice Following UVB-Induced Photodamage

As shown in Fig. 7, based on images of mice on day 20, the model and ddH₂O groups all exhibited erythema, edema, scabbing, and ulceration of the dorsal skin. However, these symptoms were significantly relieved in mice treated with OS-LL11 or Vc. Compared with the control group, epidermal thickness after UVB irradiation increased significantly by 108.10 ± 3.26 μm; in contrast, OS-LL11 treatment reduced epidermal thickness by 82.88 ± 4.17 μm (Fig. 8A, B). After UVB irradiation, dermal thickness increased by 231.30 ± 12.52 μm; however, OS-LL11 application reduced dermal thickness by 155.70 ± 13.90 μm (Fig. 8C, D). In addition, Masson's trichrome staining demonstrated that the degree of fibrosis was increased after UVB irradiation but was reversed by OS-LL11 and Vc administration (Fig. 8C).

3.7. OS-LL11 Up-Regulated SOD, GSH, and NO but Down-Regulated H_2O_2 in UVB-Damaged Mouse Skin

Levels of SOD and GSH in mouse skin decreased by 43.17% ± 3.67% and 77.23% ± 3.36%, respectively, after UVB irradiation. However, following OS-LL11 treatment, SOD and GSH increased by 34.13 ± 2.50% (Fig. 9A) and 64.16% ± 2.69% (Fig. 9B), respectively. UVB exposure led to an increase in H_2O_2 levels and decrease in NO levels in mouse skin. In contrast, OS-LL11 application resulted in a marked decrease in H_2O_2 (76.85% ± 8.18%) (Fig. 9D) and increase in NO (54.58% ± 4.01%,) (Fig. 9C). Quantitative analysis revealed that OS-LL11 treatment significantly inhibited the level of UVB-induced H_2O_2 and promoted NO production.

Fig. 10. Effects of OS-LL11 treatment on IL-1α, IL-1β, IL-6, and TNF-α levels in dorsal skin of UVB-irradiated mice.
OS-LL11 reduced the levels of IL-1α (A); IL-1β (B); IL-6 (C); and TNF-α (D) after UVB irradiation. $*P < 0.05$; $**P < 0.01$, $****P < 0.0001$ indicate significant differences. All bars represent mean ± SD of three independent experiments performed in triplicate.

3.8. OS-LL11 Decreased Levels of Inflammatory Cytokines in UVB-Irradiated Mouse Skin

Compared with the control group, the levels of IL-6, IL-1α, IL-1β, and TNF-α were up-regulated in the UVB-irradiated groups (Fig. 10). However, OS-LL11 treatment significantly inhibited the increase induced by UVB irradiation. Notably, compared to the UVB-irradiated group, IL-1α, IL-1β, IL-6, and TNF-α decreased by 68.42% ± 7.56% (Fig. 10A), 80.31% ± 7.75% (Fig. 10B), 66.50% ± 3.94% (Fig. 10C), and 78.69% ± 7.19% (Fig. 10D), respectively.

### 3.9. OS-LL11 Reduced UVB-Induced Apoptosis Protein Levels in Mouse Skin

After UVB irradiation, there was an increase in apoptosis in the dorsal skin of mice (73.46% ± 1.65%), whereas apoptosis in the OS-LL11 and Vc groups decreased by 40.44% ± 2.22% and 37.72% ± 2.41%, respectively (Fig. 11A, B). The level of 8-OHdG in UVB-irradiated mice increased by 81.23% ± 6.62%. Furthermore, after UVB irradiation, the levels of Bax and Bcl-2 increased by 84.68% ± 6.05% and decreased by 29.59% ± 3.34%, respectively. In contrast, OS-LL11 treatment resulted in a decrease in the level of 8-OHdG by 59.95% ± 6.46% (Fig. 11C) and Bax by 70.39% ± 5.82% (Fig. 11E), but an increase in Bcl-2 by 26.36% ± 4.11% (Fig. 11D).

4. Discussion

After penetrating the skin, UVB can cause considerable impairments, including DNA damage, oxidative stress, apoptosis, and other injuries [32]. Furthermore, long-term exposure to UVB irradiation can cause skin cancer and aging [33]. Antioxidants, including Vc and β-carotene, have garnered substantial attention for the management of these diseases and skin damage. However, long-term administration may cause severe side effects, such as diarrhea and nausea [34]. As a result, investigations on potential molecules for the treatment of photodamage remain crucial. Compared with traditional medicines, peptides exhibit many advantages, such as high activity, stability, and specificity, and have attracted the interest of the scientific community [35].

In this study, we identified a novel antioxidant peptide from *O. schmackeri*, and cloned the full-length cDNA sequence from the cDNA library. After a BLAST search of the NCBI database, no similar amino acid sequence was found. Therefore, we named this new peptide OS-LL11 (LLPPWLCPRNK) (Fig. 1) and explored its protective abilities (and underlying mechanisms) against UVB irradiation injury in mice and *PAM 212* cells.

Results showed that OS-LL11 had a protective effect against *PAM 212* cell viability damage induced by UVB irradiation and H_2O_2 stimulation (Fig. 3). When cells received excessive UV-B radiation, the lipid layer of the cell membrane was destroyed by UV-B, at this time, the permeability of the cell membrane was changed and the release rate of LDH was increased, therefore, detection of LDH release rate in the cell culture
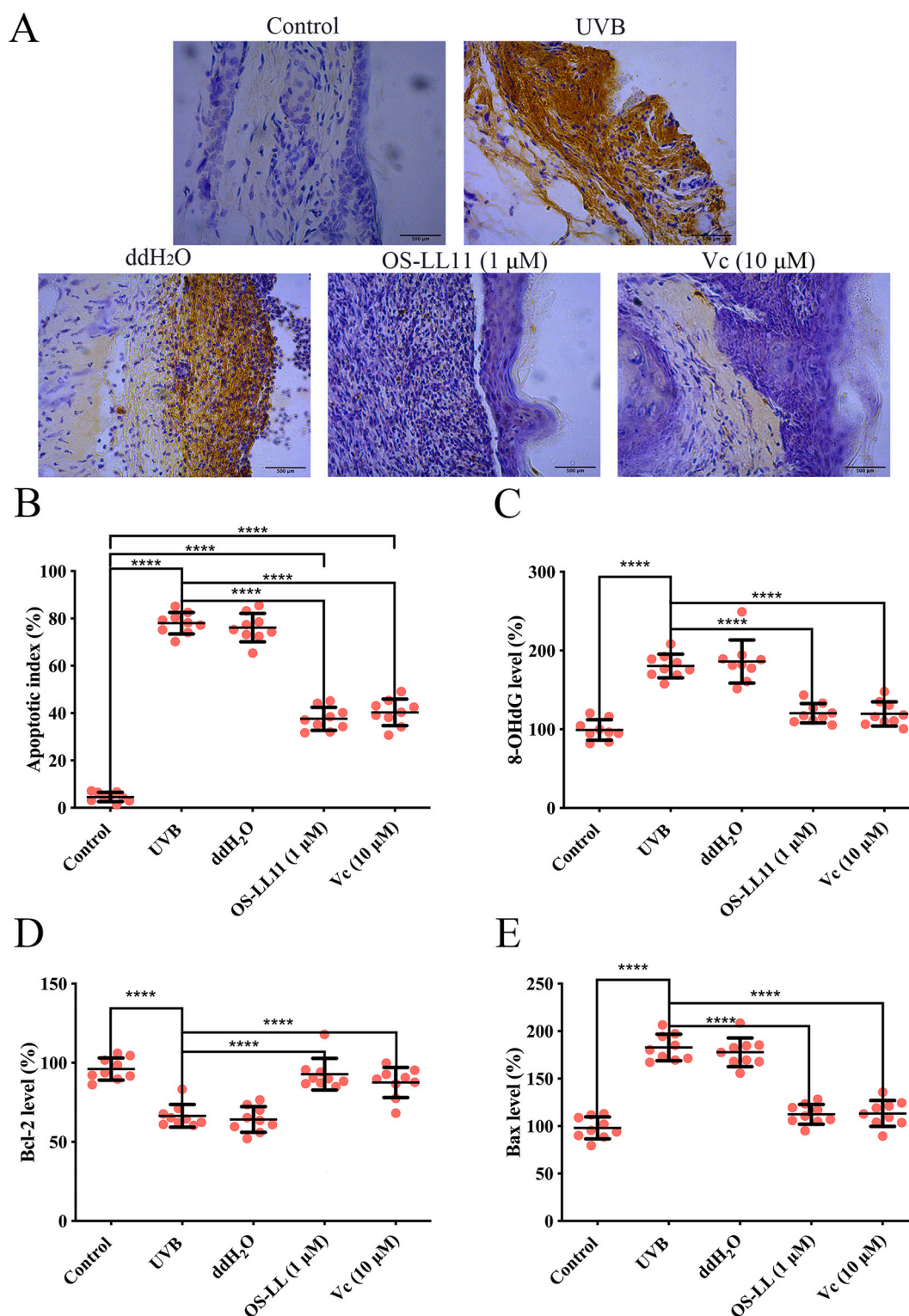
Fig. 11. Effects of OS-LL11 on apoptosis and protein levels in UVB-irradiated mouse skin.
A. Image of TUNEL staining; B. Histogram of apoptotic cells in each group; C. OS-LL11 application decreased 8-OHdG levels; D. OS-LL11 application increased Bcl-2 levels; E. OS-LL11 application decreased Bax levels. Scale bar: 500 μm. ****$P < 0.0001$ indicates significant differences. All data are means (±SD) of three independent experiments and each sample was performed in triplicate.

medium can be used to evaluate the degree of cell damage [9]. By detecting the level of endogenous antioxidants, we found that OS-LL11 significantly increased the level of CAT and decreased the levels of LPO, MDA, and LDH, thus maintaining intracellular oxidative homeostasis (Fig. 4). Based on biochemical experiments, OS-LL11 also showed

scavenging ability against ABTS$^+$ free radicals, further indicating that the peptide may play an antioxidant role (Fig. 2). We tested the effects of OS-LL11 on ROS levels in *PAM 212* cells, with OS-LL11 pretreatment shown to reduce ROS production significantly (Fig. 5), again highlighting the potential protective effects of OS-LL11 against damage

caused by UVB irradiation. To explore the antioxidant mechanism of OS-LL11 in cells, we detected oxidative stress-associated protein expression levels. Results showed that Keap1, HO-1, NQO1, and GCLM were reduced after UVB irradiation and H_2O_2 stimulation, but OS-LL11 significantly improved this inhibition (Fig. 6). These findings suggest that OS-LL11 can provide significant protection against oxidative stress caused by UVB or H_2O_2 stimulation in cells.

Next, we explored whether OS-LL11 exhibits the same photo-protective effects on UVB irradiation-induced mouse skin photodamage. After 20 days of UVB irradiation, mouse skin developed ulcerations and varying degrees of injury. However, application of OS-LL11 helped accelerate skin scab formation and promote normal skin regeneration (Fig. 7). We also confirmed the effect of the peptide on the thickening of abnormal epidermis and dermis (Fig. 8). Furthermore, Masson staining indicated that OS-LL11 helped reverse the increase in collagen fibers induced by UVB irradiation (Fig. 8C). Thus, OS-LL1 showed considerable protective effects against photodamage in animal experiments. Therefore, we not only observed a protective effect of the peptide in vitro but also a restorative effect in vivo. This emphasized the protection of OS-LL11 to resist UV-induced damage.

Given the above results, we also explored the related protective mechanism of OS-LL11. UVB irradiation induces the expression of oxidative stress-related transcription factors, such as nuclear factor (NF)-kB [36]. These transcription factors further cause the expression of pro-inflammatory cytokines, resulting in photo-aging and photodamage by modulating the levels of certain matrix metalloprotein (MMP) family members [37]. IL-1α, IL-1β, IL-6, and TNF-α are known to have important effects on UVB irradiation-induced MMP-1 overexpression [38,39]. Consequently, we investigated changes in the levels of IL-1α, IL-1β, IL-6, and TNF-α following OS-LL11 administration after UVB irradiation. Results demonstrated that the expression levels of these pro-inflammatory cytokines were significantly down-regulated in UVB-stimulated mice after OS-LL11 application, thus highlighting its photo-protective effects (Fig. 10).

UV radiation appears to have different effects on organisms. On the one hand, UV radiation can increase the levels of endogenous antioxidants in a variety of organisms, especially aquatic animals and amphibians, such as *Tigriopus japonicus*, sea urchin larvae, *Bufo arenarum* tadpoles, and *Ambystoma maculatum* embryos [40]. On the other hand, excessive UV radiation can consume antioxidants in mammals, such as mice and guinea pigs, resulting in a decrease in antioxidants in vivo [41]. The discrepant effects may be due to different doses and times of UV radiation in different organisms. In the current study, OS-LL11 application improved the levels of SOD, GSH, and NO (Fig. 9A, B). Therefore, the protective effect of OS-LL11 against photodamage may be achieved by increasing the level of antioxidants in the body and cells. SOD is an important endogenous antioxidant enzyme in the body that fights against oxidative stress [42]. GSH is involved in the detoxification of a variety of toxins, and CAT can decompose and transform H_2O_2 in the body [43]. Therefore, normal levels of SOD, GSH, CAT, and H_2O_2 are important for the body to maintain oxidative homeostasis [42,43]. Therefore, we explored the effects of UV radiation on antioxidants in mouse skin and keratinocytes, as well as the protective effects of OS-LL11 on these tissues and cells.

Excessive UV radiation will cause skin damage [43]. Importantly, the formation of DNA damage is also the main consequence of organisms exposed to excessive ultraviolet radiation, and UV-induced DNA cross-links usually produce pyrimidine dimer as the thymine–thymine cyclo-butane (T–T) dimer and thymine–thymine pyrimidine–pyrimidone (6–4) (T (6–4) T) photoproduct. [44,45]. As a marker of DNA oxidative damage, 8-OHdG expression is also closely related to apoptosis and positively correlated with the degree of DNA damage [46]. High 8-OHdG expression can also affect the activation of downstream DNA repair-related signaling pathways, e.g., changes in Bax and BCL-2 protein levels induced by p53 [29]. Several studies have found that small molecular peptides can protect against apoptosis. For example, local

application of *O. margaretae*-derived OM-GL15 on the skin of mice reduces the protein levels of p53, caspase 3, and caspase 9 [29]. In this study, we found that OS-LL11 had an effect on the level of 8-OHdG and activation of the Bax/BCL-2 signaling pathway in the UVB-induced mouse skin injury model, thus highlighting the potential role of this peptide in protecting cells and tissues from DNA damage (Fig. 11).

Amphibian-derived peptides are an important source of anti-photodamage peptides. Many antioxidant peptides have been found to have protective effects on skin damage caused by UV radiation. For example, peptides FW1 and FW2 from *Hyla annectans* protect skin by inhibiting the secretion of inflammatory factors such as TNF-α and activating the MAPK signaling pathway [21]. OM-GL15, a polypeptide from *O. margaretae*, resists UVB-induced skin injury by inhibiting the production of apoptosis-related proteins [29]. Although a variety of anti-photo injury peptides have been reported, novel peptide identification and development remain crucial.

In this study, a novel polypeptide (OS-LL11) was identified from *O. schmackeri*. Its protective mechanisms, including balancing the redox system and inhibiting the production of apoptotic proteins and inflammatory factors, suggest that OS-LL11 could be a new and useful protective peptide against photodamage. Although we partially explored the protective effects of OS-LL11 against photodamage, due to the complex mechanisms underlying intracellular signaling pathways, its specific transfer pathways and interactions require further study.

CRediT authorship contribution statement

Chun Xie: Writing - original draft, Methodology, Software. **Yan Fan**: Writing - original draft, Methodology, Software. **Saige Yin**: Writing - original draft, Methodology, Software, Writing - review & editing, Supervision. **Yilin Li**: Methodology. **Naixin Liu**: Software. **Yixinag Liu**: Software. **Longjun Shu**: Data curation. **Zhe Fu**: Investigation. **Yinglei Wang**: Investigation. **Yue Zhang**: Visualization. **Xiaojie Li**: Visualization. **Ying Wang**: Conceptualization, Funding acquisition. **Jun Sun**: Conceptualization, Funding acquisition. **Xinwang Yang**: Writing - review & editing, Supervision, Conceptualization, Funding acquisition.

Declaration of Competing Interest

The authors declare that there are no conflicts of interest regarding the publication of this paper.

Acknowledgements

References

[1] J. Fuchs, Potentials and limitations of the natural antioxidants RRR-alpha-tocopherol, L-ascorbic acid and beta-carotene in cutaneous photoprotection, Free Radic. Biol. Med. 25 (1998) 848–873.

[2] Y. Miyachi, Photoaging from an oxidative standpoint, J. Dermatol. Sci. 9 (1995) 79–86.

[3] C. Lee, G.H. Park, E.M. Ahn, B.A. Kim, C.I. Park, J.H. Jang, Protective effect of *Codium fragile* against UVB-induced pro-inflammatory and oxidative damages in HaCaT cells and BALB/c mice, Fitoterapia 86 (2013) 54–63.

[4] L. Subedi, T.H. Lee, H.M. Wahedi, S.H. Baek, S.Y. Kim, Corrigendum to "resveratrol-enriched Rice attenuates UVB-ROS-induced skin aging via Downregulation of inflammatory cascades", Oxidative Med. Cell. Longev. 2018 (2018) 6052623.

[5] M. Ichihashi, M. Ueda, A. Budiyanto, T. Bito, M. Oka, M. Fukunaga, K. Tsuru, T. Horikawa, UV-induced skin damage, Toxicology 189 (2003) 21–39.

[6] D.E. Heck, A.M. Vetrano, T.M. Mariano, J.D. Laskin, UVB light stimulates production of reactive oxygen species: unexpected role for catalase, J. Biol. Chem. 278 (2003) 22432–22436.

[7] S.F. Retta, P. Chiarugi, L. Trabalzini, P. Pinton, A.M. Belkin, Reactive oxygen species: friends and foes of signal transduction, J. Signal Transduct. 2012 (2012) 534029.

[8] A. Glady, M. Tanaka, C.S. Moniaga, M. Yasui, M. Hara-Chikuma, Involvement of NADPH oxidase 1 in UVB-induced cell signaling and cytotoxicity in human keratinocytes, Biochem. Biophys. Rep. 14 (2018) 7–15.

[9] S. Yin, Y. Wang, N. Liu, M. Yang, Y. Hu, X. Li, Y. Fu, M. Luo, J. Sun, X. Yang, Potential skin protective effects after UVB irradiation afforded by an antioxidant peptide from *Odorrana andersonii*, Biomed. Pharmacother. 120 (2019) 109535.

[10] C. Alonso, L. Rubio, S. Tourino, M. Marti, C. Barba, F. Fernandez-Campos, L. Coderch, J.L. Parra, Antioxidative effects and percutaneous absorption of five polyphenols, Free Radic. Biol. Med. 75 (2014) 149–155.

[11] D.H. McDaniel, J.M. Waugh, L.I. Jiang, T.J. Stephens, A. Yaroshinsky, C. Mazur, M. Wortzman, D.B. Nelson, Evaluation of the antioxidant capacity and protective effects of a comprehensive topical antioxidant containing water-soluble, enzymatic, and lipid-soluble antioxidants, J. Clin. Aesthet. Dermatol. 12 (2019) 46–53.

[12] L. Baumann, D.K. Duque, M.J. Schirripa, Split-face vitamin C consumer preference study, J. Drugs Dermatol. 13 (2014) 1208–1213.

[13] R.J.B. Kohen, Skin antioxidants: their role in aging and in oxidative stress–new approaches for their evaluation, Pharmacotherapy 53 (1999) 181.

[14] E. Esposito, D. Rotilio, V. Di Matteo, C. Di Giulio, M. Cacchio, S. Algeri, A review of specific dietary antioxidants and the effects on biochemical mechanisms related to neurodegenerative processes, Neurobiol. Aging 23 (2002) 719–735.

[15] X. Yang, Y. Wang, Y. Zhang, W.H. Lee, Y. Zhang, Rich diversity and potency of skin antioxidant peptides revealed a novel molecular basis for high-altitude adaptation of amphibians, Sci. Rep. 6 (2016) 19866.

[16] Y. Zhang, Q.Q. Wang, Z. Zhao, C.J. Deng, Animal secretory endolysosome channel discovery, Zool. Res. 42 (2021) 141–152.

[17] B.T. Clarke, The natural history of amphibian skin secretions, their normal functioning and potential medical applications, Biol. Rev. Camb. Philos. Soc. 72 (1997) 365–379.

[18] M. Zasloff, Antimicrobial peptides of multicellular organisms: my perspective, Adv. Exp. Med. Biol. 1117 (2019) 3–6.

[19] H. Yang, X. Wang, X. Liu, J. Wu, C. Liu, W. Gong, Z. Zhao, J. Hong, D. Lin, Y. Wang, R. Lai, Antioxidant peptidomics reveals novel skin antioxidant system, Mol. Cell. Proteomics 8 (2009) 571–583.

[20] R. Spinelli, I. Sanchis, F.M. Aimaretti, A.M. Attademo, M. Portela, M.V. Humpola, G.G. Tonarelli, A.S. Siano, Natural multi-target inhibitors of Cholinesterases and monoamine oxidase enzymes with antioxidant potential from skin extracts of *Hypsiboas cordobae* and *Pseudis minuta* (Anura: Hylidae), Chem. Biodivers. 16 (2019), e1800472.

[21] H. Liu, X. Guo, T. Yi, Y. Zhu, X. Ren, R. Guo, Y. Dai, S. Liang, Frog skin derived peptides with potential protective effects on ultraviolet B-induced cutaneous Photodamage, Front. Immunol. 12 (2021) 613365.

[22] W.Y. Liu, J.T. Zhang, T. Miyakawa, G.M. Li, R.Z. Gu, M. Tanokura, Antioxidant properties and inhibition of angiotensin-converting enzyme by highly active peptides from wheat gluten, Sci. Rep. 11 (2021) 5206.

[23] I. Sanchis, R. Spinelli, N. Aschemacher, M.V. Humpola, A. Siano, Acetylcholinesterase inhibitory activity of a naturally occurring peptide isolated from *Boana pulchella* (Anura: Hylidae) and its analogs, Amino Acids 52 (2020) 387–396.

[24] X. Cao, Y. Wang, C. Wu, X. Li, Z. Fu, M. Yang, W. Bian, S. Wang, Y. Song, J. Tang, X. Yang, Cathelicidin-OA1, a novel antioxidant peptide identified from an amphibian, accelerates skin wound healing, Sci. Rep. 8 (2018) 943.

[25] D. Qin, W.H. Lee, Z. Gao, W. Zhang, M. Peng, T. Sun, Y. Gao, Protective effects of antioxidin-RL from *Odorrana livida* against ultraviolet B-irradiated skin photoaging, Peptides 101 (2018) 124–134.

[26] S. Yin, S. Li, W. Bian, M. Yang, X.J.I.J.O.P.R. Yang, Therapeutics, antioxidant peptide AOP-P1 derived from odorous frog showed protective effects against UVB-induced skin damages, Int. J. Pept. Res. Ther. 26 (2019) 557–565.

[27] X. Yang, W.H. Lee, Y. Zhang, Extremely abundant antimicrobial peptides existed in the skins of nine kinds of Chinese odorous frogs, J. Proteome Res. 11 (2012) 306–319.

[28] Y. Wang, Z. Feng, M. Yang, L. Zeng, B. Qi, S. Yin, B. Li, Y. Li, Z. Fu, L. Shu, C. Fu, P. Qin, Y. Meng, X. Li, Y. Yang, J. Tang, X. Yang, Discovery of a novel short peptide with efficacy in accelerating the healing of skin wounds, Pharmacol. Res. 163 (2021) 105296.

[29] X. Zhang, C. Feng, S. Wang, Y. Wang, Z. Fu, Y. Zhang, H. Sun, C. Xie, Y. Fu, J. Tao, M. Luo, X. Yang, A novel amphibian-derived peptide alleviated ultraviolet B-induced photodamage in mice, Biomed. Pharmacother. 136 (2021) 111258.

[30] R. Re, N. Pellegrini, A. Proteggente, A. Pannala, M. Yang, C. Rice-Evans, Antioxidant activity applying an improved ABTS radical cation decolorization assay, Free Radic. Biol. Med. 26 (1999) 1231–1237.

[31] K.C. Wen, H.H. Chiu, P.C. Fan, C.W. Chen, S.M. Wu, J.H. Chang, H.M. Chiang, Antioxidant activity of *Ixora parviflora* in a cell/cell-free system and in UV-exposed human fibroblasts, Molecules 16 (2011) 5735–5752.

[32] S. Ramachandran, N. Rajendra Prasad, S. Karthikeyan, Sesamol inhibits UVB-induced ROS generation and subsequent oxidative damage in cultured human skin dermal fibroblasts, Arch. Dermatol. Res. 302 (2010) 733–744.

[33] J. D'Orazio, S. Jarrett, A. Amaro-Ortiz, T. Scott, UV radiation and the skin, Int. J. Mol. Sci. 14 (2013) 12222–12248.

[34] B. Yin, S. Tang, J. Sun, X. Zhang, J. Xu, L. Di, Z. Li, Y. Hu, E. Bao, Vitamin C and sodium bicarbonate enhance the antioxidant ability of H9C2 cells and induce HSPs to relieve heat stress, Cell Stress Chaperones 23 (2018) 735–748.

[35] X. Li, Y. Wang, Z. Zou, M. Yang, C. Wu, Y. Su, J. Tang, X. Yang, OM-LV20, a novel peptide from odorous frog skin, accelerates wound healing in vitro and in vivo, Chem. Biol. Drug Des. 91 (2018) 126–136.

[36] M. Rahman, J.K. Kundu, J.W. Shin, H.K. Na, Y.J. Surh, Docosahexaenoic acid inhibits UVB-induced activation of NF-kappaB and expression of COX-2 and NOX-4 in HR-1 hairless mouse skin by blocking MSK1 signaling, PLoS One 6 (2011), e28065.

[37] S. Kondo, The roles of cytokines in photoaging, J. Dermatol. Sci. 23 (Suppl. 1) (2000) S30–S36.

[38] C.H. Park, M.J. Lee, J. Ahn, S. Kim, H.H. Kim, K.H. Kim, H.C. Eun, J.H. Chung, Heat shock-induced matrix metalloproteinase (MMP)-1 and MMP-3 are mediated through ERK and JNK activation and via an autocrine interleukin-6 loop, J. Invest Dermatol. 123 (2004) 1012–1019.

[39] M. Wlaschek, K. Bolsen, G. Herrmann, A. Schwarz, F. Wilmroth, P.C. Heinrich, G. Goerz, K. Scharffetter-Kochanek, UVA-induced autocrine stimulation of fibroblast-derived-collagenase by IL-6: a possible mechanism in dermal photodamage? J. Invest Dermatol. 101 (1993) 164–168.

[40] P. Feher, Z. Ujhelyi, J. Varadi, F. Fenyvesi, E. Roka, B. Juhasz, B. Varga, M. Bombicz, D. Priksz, I. Bacskay, M. Vecsernyes, Efficacy of pre- and post-treatment by topical formulations containing dissolved and suspended *Silybum marianum* against UVB-induced oxidative stress in guinea pig and on HaCaT keratinocytes, Molecules 21 (2016).

[41] A.R. Im, S.H. Yeon, J.S. Lee, K.A. Um, Y.J. Ahn, S. Chae, Protective effect of fermented Cyclopia intermedia against UVB-induced damage in HaCaT human keratinocytes, BMC Complement. Altern. Med. 16 (2016) 261.

[42] M. Deng, Y. Xu, Z. Yu, X. Wang, Y. Cai, H. Zheng, W. Li, W. Zhang, Protective effect of fat extract on UVB-induced photoaging in vitro and in vivo, Oxidative Med. Cell. Longev. 2019 (2019) 6146942.

[43] R.O. de Souza, G. de Assis Dias Alves, A.L.S. Aguillera, H. Rogez, M.J.V. Fonseca, Photochemoprotective effect of a fraction of a partially purified extract of *Byrsonima crassifolia* leaves against UVB-induced oxidative stress in fibroblasts and hairless mice, J. Photochem. Photobiol. B 178 (2018) 53–60.

[44] V.K. Yadav, P. Awasthi, A. Kumar, Detection of UV-induced thymine dimers, Methods Mol. Biol. 2031 (2019) 313–322.

[45] T. Douki, The variety of UV-induced pyrimidine dimeric photoproducts in DNA as shown by chromatographic quantification methods, Photochem. Photobiol. Sci. 12 (2013) 1286–1302.

[46] J.K. Lee, S.H. Ko, S.K. Ye, M.H. Chung, 8-Oxo-2′-deoxyguanosine ameliorates UVB-induced skin damage in hairless mice by scavenging reactive oxygen species and inhibiting MMP expression, J. Dermatol. Sci. 70 (2013) 49–57.